

Phenylbutyric acid inhibits epithelial-mesenchymal transition during bleomycin-induced lung fibrosis



Hui Zhao^{b,1,**}, Hou-Ying Qin^{b,1}, Lin-Feng Cao^b, Yuan-Hua Chen^a, Zhu-Xia Tan^b, Cheng Zhang^a, De-Xiang Xu^{a,*}

^a Department of Toxicology, Anhui Medical University, Hefei 230032, China

^b Second Affiliated Hospital, Anhui Medical University, Hefei 230601, China

HIGHLIGHTS

- UPR signaling is activated in the pathogenesis of BLM-induced pulmonary fibrosis.
- PBA, an ER chemical chaperone, inhibits BLM-evoked UPR activation in the lungs.
- PBA inhibits BLM-induced pulmonary NF-κB activation in mice.
- PBA alleviates BLM-induced epithelial mesenchymal transition and lung fibrosis.

ARTICLE INFO

Article history:

Received 9 September 2014

Received in revised form 7 October 2014

Accepted 12 October 2014

Available online 18 October 2014

Keywords:

Phenylbutyric acid

Bleomycin

Endoplasmic reticulum stress

Unfolded protein response

Epithelial-mesenchymal transition

ABSTRACT

A recent report showed that unfolded protein response (UPR) signaling was activated during bleomycin (BLM)-induced pulmonary fibrosis. Phenylbutyric acid (PBA) is an endoplasmic reticulum (ER) chemical chaperone that inhibits the UPR signaling. The present study investigated the effects of PBA on BLM-induced epithelial-mesenchymal transition (EMT) and pulmonary fibrosis. For induction of pulmonary fibrosis, all mice except controls were intratracheally injected with a single dose of BLM (3.0 mg/kg). In PBA+BLM group, mice were intraperitoneally injected with PBA (150 mg/kg) daily. Three weeks after BLM injection, EMT was measured and pulmonary fibrosis was evaluated. BLM-induced pulmonary UPR activation was inhibited by PBA. Moreover, BLM-induced pulmonary nuclear factor kappa B (NF-κB) p65 activation was blocked by PBA. In addition, BLM-induced up-regulation of pulmonary inflammatory cytokines was repressed by PBA. Further analysis showed that BLM-induced α -smooth muscle actin (α -SMA), a marker for EMT, was significantly attenuated by PBA. Moreover, BLM-induced pulmonary collagen (Col1 α 1 and Col1 α 2) was obviously inhibited by PBA. Importantly, BLM-induced pulmonary fibrosis, as determined using Sirius red staining, was obviously alleviated by PBA. Taken together, these results suggest that PBA alleviates ER stress-mediated EMT in the pathogenesis of BLM-induced pulmonary fibrosis.

© 2014 Elsevier Ireland Ltd. All rights reserved.

1. Introduction

Idiopathic pulmonary fibrosis, characterized by fibroblast proliferation and extracellular matrix remodeling, is a chronic pulmonary disease of unknown origin ultimately leading to death

(Borchers et al., 2011; King et al., 2011). Bleomycin (BLM), a widely used antineoplastic drug, causes a dose-dependent interstitial pulmonary fibrosis (Adamson and Bowden, 1974). Intratracheal instillation of BLM into the lungs of rodent animals causes alveolar cell damage, an inflammatory response, epithelial-mesenchymal transition (EMT) and subsequent extracellular matrix deposition, resembling human interstitial pulmonary fibrosis (Moore and Hogaboam, 2008). BLM-induced pulmonary fibrosis has been the most commonly used model for idiopathic pulmonary fibrosis (Moeller et al., 2008). Nevertheless, the mechanisms of BLM-induced pulmonary fibrosis are not completely understood.

* Corresponding author. Tel.: +86 551 65167923; fax: +86 551 65161179.

** Corresponding author.

E-mail addresses: zhaohuichenxi@126.com (H. Zhao), xudex@126.com (D.-X. Xu).

¹ These authors contributed equally to this work.

Endoplasmic reticulum (ER) is an important organelle required for normal cellular function. In the ER, nascent proteins are folded with the assistance of ER chaperones. Accumulation of unfolded and misfolded proteins aggregated in the ER lumen causes ER stress and activation of a signal response termed unfolded protein response (UPR) (Wu and Kaufman, 2006). The UPR signaling is mediated by three transmembrane ER proteins: inositol requiring ER-to-nucleus signal kinase (IRE) 1, activating transcription factor (ATF) 6 and double-stranded RNA-activated kinase (PKR)-like ER kinase (PERK) (Kohno, 2007). An earlier report showed that the level of processed p50 ATF6 and spliced x-box binding protein (sXBP)-1, a downstream molecule of IRE1 pathway, was significantly increased in the lungs of IPF patients (Lawson et al., 2008). Two recent studies found that pulmonary UPR signaling was activated in the pathogenesis of BLM-induced pulmonary fibrosis (Lawson et al., 2011; Zhong et al., 2011).

Phenylbutyric acid (PBA) is a low molecular weight fatty acid that has been used for treatment of urea cycle disorders in children and sickle cell disease (Burlina et al., 2001). Numerous studies have demonstrated that PBA acts as a chemical chaperone that inhibits ER stress and UPR signaling activation (Basseri et al., 2009). Indeed, PBA could attenuate ER stress and restore glucose homeostasis in a mouse model of type 2 diabetes (Ozcan et al., 2006). Moreover, PBA inhibits UPR signaling activation and protects against leptin resistance in the hypothalamus of obese mice (Ozcan et al., 2009). Recently, we showed that PBA not only significantly attenuated ER stress but also inhibited fructose-evoked hepatic SREBP-1c activation and lipid accumulation (Zhang et al., 2012). In humans, PBA partially alleviated lipid-induced insulin resistance and β -cell dysfunction (Xiao et al., 2011). According to a recent report, pretreatment with PBA significantly reduced ischemia-reperfusion-induced inflammation, apoptosis and necrosis, and improved liver regeneration through inhibiting UPR signaling activation (Ben Mosbah et al., 2010). Nevertheless, whether PBA protects against BLM-induced pulmonary fibrosis remains to be determined.

The aim of the present study was to investigate the effects of PBA on BLM-induced EMT and pulmonary fibrosis in mice. We demonstrate for the first time that PBA inhibits not only BLM-induced pulmonary ER stress but also pulmonary inflammation and subsequent EMT in the pathogenesis of BLM-induced lung fibrosis. Moreover, PBA effectively protects against BLM-induced pulmonary fibrosis in mice.

2. Materials and methods

2.1. Chemicals and reagents

BLM and PBA were purchased from Sigma Chemical Co., (St. Louis, MO). GRP78, IRE1 α , phosphor-IRE1 α , C/EBP homologous protein (CHOP), and phosphor-eukaryotic initiation factor 2 α (eIF2 α) antibodies were from Cell Signaling Technology (Beverly, MA). NF- κ B p65, α -smooth muscle actin (α -SMA) and β -actin antibodies, horseradish peroxidase-conjugated goat anti-rabbit, goat anti-mouse and anti-donkey anti-goat IgGs were from Santa Cruz Biotechnology, Inc., (Santa Cruz, CA). TRI reagent was purchased from Molecular Research Center, Inc., (Cincinnati, OH), RNase-free DNase, AMV and GoTaq[®] qPCR master mix were from Promega Corporation (Madison, WI). All specific primers were synthesized by Life Technologies Corporation (Carlsbad, CA). Chemiluminescence (ECL) detection kits were obtained from Thermo Fisher Scientific Inc., (Rockford, IL). Polyvinylidene fluoride (PVDF) membrane was from Millipore Corporation (Belford, MA). All other reagents were purchased from Sigma Chemical Co., (St. Louis, MO) if not otherwise stated.

2.2. Animals and treatments

Adult female CD-1 mice (8 week-old, 28–32 g) were purchased from Beijing Vital River whose foundation colonies were all introduced from Charles River Laboratories, Inc. The animals were allowed free access to food and water at all times and maintained on a 12 h light/dark cycle in a controlled temperature (20–25 °C) and humidity (50 \pm 5%) environment. For the induction of pulmonary fibrosis, mice were intratracheally injected with a single dose of BLM (3.0 mg/kg body weight in 50 μ L phosphate buffered saline). The doses of BLM used in the present study referred to others (Zhao et al., 2014). To investigate the effects of PBA on BLM-induced pulmonary fibrosis, mice were intraperitoneally (i.p.) injected with PBA (150 mg/kg) daily, beginning at 30 min before BLM. The doses of PBA used in the present study referred to others (Zhang et al., 2012). Control mice received an i.p. injection of NS daily. All mice were euthanized by exsanguination during pentobarbital anesthesia (75 mg/kg, i.p.) three weeks after BLM injection. Lung fibrosis was assessed by Sirius red staining as well as lung histology. Some lung samples were collected and kept at –80 °C for subsequent immunoblots and real-time RT-PCR. This study was approved by the Association of Laboratory Animal Sciences and the Center for Laboratory Animal Sciences at Anhui Medical University (Permit Number: 13-0016). All procedures on animals followed the guidelines for humane treatment set by the Association of Laboratory Animal Sciences and the Center for Laboratory Animal Sciences at Anhui Medical University.

2.3. Pulmonary histology

Lung tissues were fixed in 4% formalin and embedded in paraffin according to the standard procedure. Paraffin-embedded lung tissues were serially sectioned. At least five consecutive longitudinal sections were stained with hematoxylin and eosin (H and E) and scored for the extent of pathology on a scale of 0–5, where 0 was defined as no lung abnormality, and 1, 2, 3, 4, and 5 were defined as the presence of inflammation involving 10%, 10–30%, 30–50%, 50–80%, or >80% of the lungs, respectively. Lung fibrosis was evaluated by Sirius red staining for collagen accumulation. The percentages of collagen deposition areas were quantified using NIH ImageJ software (<http://rsb.info.nih.gov/ij/>).

2.4. Immunoblots

Total pulmonary lysate was prepared by homogenizing 50 mg lung tissue in 300 μ L lysis buffer (50 mM Tris–HCl, pH 7.4, 150 mM NaCl, 1 mM EDTA, 1% Triton X-100, 1% sodium deoxycholate, 0.1% sodium dodecylsulfate, 1 mM phenylmethylsulfonyl fluoride) supplemented with a cocktail of protease inhibitors (Roche). For nuclear protein extraction, total pulmonary lysate was suspended in hypotonic buffer and then kept on ice for 15 min. The suspension was then mixed with detergent and centrifuged for 30 s at 14,000 \times g. Protein concentrations were determined with bicinchoninic acid (BCA) protein assay reagents (Pierce, Rockford, IL) according to manufacturer's instructions. For immunoblots, same amount of protein (30–60 μ g) was separated electrophoretically by SDS-PAGE and transferred to a polyvinylidene fluoride membrane. The membranes were incubated for 2 h with the following antibodies: α -SMA, CHOP, GRP78, phosphor-IRE1 α , IRE1 α and phosphor-eIF2 α . For total proteins, β -actin was used as a loading control. After washes in DPBS containing 0.05% Tween-20 four times for 10 min each, the membranes were incubated with goat anti-rabbit IgG or goat anti-mouse antibody for 2 h. The membranes were then washed for four times in DPBS containing 0.05% Tween-20 for 10 min each, followed by signal development using an ECL

Table 1

Oligonucleotide sequence of primers for RT-PCR.

Genes	Forward (5'-3')	Reverse (5'-3')
18S	GTAACCGTTGAACCCATT	CCATCCAATCGGTAGTAGCG
TNF- α	CCCTCTGGCCAACGGCATG	TCGGGGCAGCCTTGTCCCTT
IL-1 β	GCCTCGTGTCTGCGACCCATAT	TCCTTTAGAGCCCAAGGCCACA
IFN- γ	GCTGTTACTGCCACGGCACAGT	CACCATCCTTTTGCCAGTTCCTCC
TGF- β 1	TTCCGCTGCTACTGCAAGTCA	GGGTAGCGATCGAGTGTCCA
Col 1 α 1	CAATGGCAGCGTGTGTGCG	AGCACTGCCTCCCGTCTT
Col 1 α 2	CTCATACAGCCGCGCCAGG	AGCAGGCGCATGAAGGCGAG

detection kit. The density of the specific bands was quantified using NIH ImageJ software (<http://rsb.info.nih.gov/ij/>).

2.5. Isolation of total RNA and real-time RT-PCR

Total RNA was extracted using TRI reagent. RNase-free DNase-treated total RNA (1.0 μ g) was reverse-transcribed with AMV. Real-time RT-PCR was performed with a GoTaq[®] qPCR master mix using gene-specific primers as listed in Table 1. The amplification reactions were carried out on a LightCycler[®] 480 Instrument (Roche Diagnostics GmbH, Mannheim, Germany) with an initial hold step (95 °C for 5 min) and 50 cycles of a three-step PCR (95 °C for 15 s, 60 °C for 15 s, 72 °C for 30 s). The comparative CT-method was used to determine the amount of target, normalized to an endogenous reference (18 s) and relative to a calibrator ($2^{-\Delta\Delta Ct}$) using the Lightcycler 480 software (Roche, version 1.5.0). All RT-PCR experiments were performed in triplicate.

2.6. Immunohistochemistry

For immunohistochemistry, paraffin-embedded lung sections were deparaffinized and rehydrated in a graded ethanol series. After antigen retrieval and quenching of endogenous peroxidase, sections were incubated with either α -SMA or NF- κ B p65 monoclonal antibody (1:200 dilution) at 4 °C overnight. The color reaction was developed with HRP-linked polymer detection system and counterstaining with hematoxylin.

2.7. Statistical analysis

Normally distributed data were expressed as means \pm SEM. ANOVA and the Student–Newmann–Keuls post hoc test were used to determine differences among different groups. Data that were not normally distributed were assessed for significance using non-parametric tests techniques (Kruskal–Wallis test and Mann–Whitney U test). $P < 0.05$ was considered to indicate statistical significance.

3. Results

3.1. PBA inhibits BLM-induced pulmonary ER stress

The effects of PBA on BLM-induced pulmonary ER stress were analyzed. As shown in Fig. 1A, pulmonary GRP78, an ER chaperone and a downstream target of ATF6, was up-regulated in BLM-treated mice. PBA markedly inhibited BLM-induced up-regulation of GRP78 in the lungs. C/EBP homologous protein (CHOP) and eukaryotic initiation factor 2 α (eIF2 α) are downstream targets of

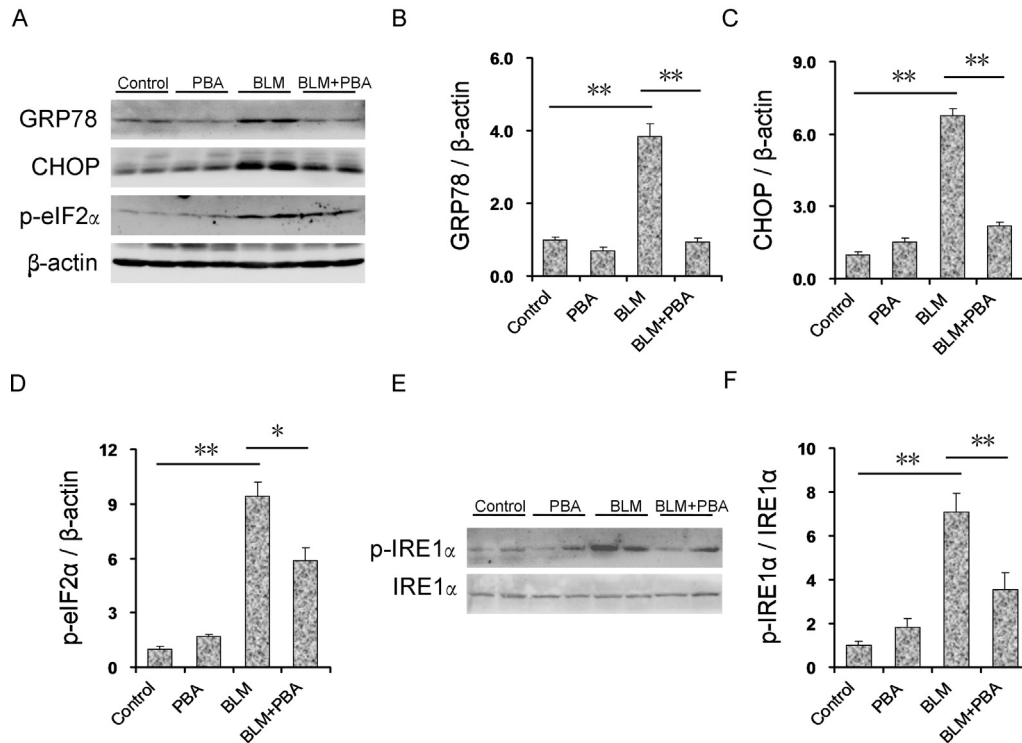


Fig. 1. Effects of PBA on BLM-induced pulmonary ER stress. In BLM group, mice were intratracheally injected with a single dose of BLM (3.0 mg/kg body weight in 50 μ L phosphate buffered saline). In BLM + PBA group, mice were intratracheally injected with BLM in combination with PBA (150 mg/kg, i.p., daily). Lungs were collected 21 days after BLM. (A) Pulmonary GRP78, CHOP and p-eIF2 α were detected by immunoblots. (B–D) Quantitative analyses of scanning densitometry on four different samples were performed. All proteins were normalized to β -actin level in the same samples. (B) GRP78. (C) CHOP. (D) p-eIF2 α . (E and F) Pulmonary IRE1 α and p-IRE1 α were detected by immunoblots. Quantitative analyses of scanning densitometry on four different samples were performed. All proteins were normalized to IRE1 α level in the same samples. All data were expressed as means \pm SEM ($n = 4$). * $P < 0.05$, ** $P < 0.01$.

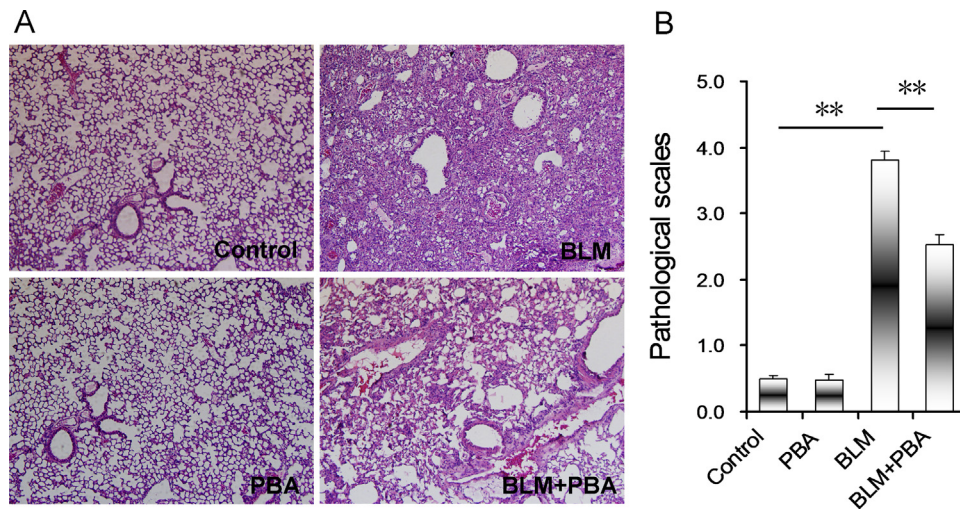


Fig. 2. Effects of PBA on BLM-induced pulmonary pathohistological damage. In BLM group, mice were intratracheally injected with a single dose of BLM (3.0 mg/kg body weight in 50 μ L phosphate buffered saline). In BLM + PBA group, mice were intratracheally injected with BLM in combination with PBA (150 mg/kg, i.p., daily). Lungs were collected 21 days after BLM. (A) Lung cross sections were stained with H and E. Original magnification: 100 \times . (B) Pathohistological scores were evaluated according to pulmonary inflammation. All data were expressed as means \pm SEM ($n = 12$). ** $P < 0.01$.

the PERK pathway. As shown in Fig. 1B, pulmonary CHOP was markedly up-regulated in BLM-treated mice. Moreover, phosphorylated eIF2 α in the lung was increased in BLM-treated mice (Fig. 1C). PBA significantly attenuated BLM-induced up-regulation of CHOP and eIF2 α phosphorylation in the lungs. The effects of PBA on pulmonary IRE1 pathway were then analyzed. As shown in Fig. 1D, the level of phosphorylated IRE1 α in the lungs was significantly increased in BLM-treated mice. PBA significantly attenuated BLM-induced pulmonary IRE1 α phosphorylation (Fig. 1D).

3.2. PBA alleviates BLM-induced pulmonary histological damage

The effects of PBA on BLM-induced pulmonary histological damage were analyzed. An obvious pulmonary edema was observed in BLM-treated mice (data not shown). Histological

examination showed an infiltration of numerous inflammatory cells in the lungs (Fig. 2A and B). PBA significantly attenuated BLM-induced pulmonary edema (data not shown). Moreover, PBA significantly alleviated BLM-induced infiltration of inflammatory cells in the lungs.

3.3. PBA inhibits BLM-induced pulmonary NF- κ B activation

The effects of PBA on BLM-induced pulmonary NF- κ B activation were analyzed. Immunohistochemistry showed that numerous NF- κ B p65-positive cells were observed in the lungs of BLM-treated mice (Fig. 3A). Further analysis showed that the number of NF- κ B p65-positive cells was significantly elevated in the lungs of BLM-treated mice (Fig. 3B). PBA markedly inhibited BLM-induced NF- κ B activation in the lungs (Fig. 3A and B).

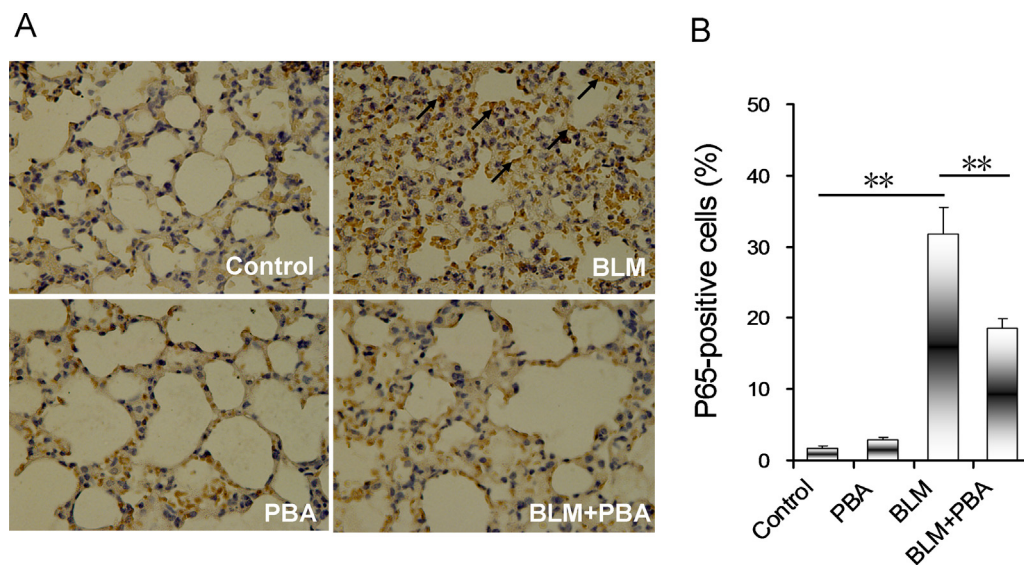


Fig. 3. Effects of PBA on BLM-induced pulmonary NF- κ B activation. In BLM group, mice were intratracheally injected with a single dose of BLM (3.0 mg/kg body weight in 50 μ L phosphate buffered saline). In BLM + PBA group, mice were intratracheally injected with BLM in combination with PBA (150 mg/kg, i.p., daily). Lungs were collected 21 days after BLM. Pulmonary nuclear translocation of NF- κ B p65 was analyzed using immunohistochemistry. (A) Representative photomicrographs of pulmonary histological specimens from mice treated with saline, PBA alone, BLM alone and BLM plus PBA. Original magnification: 400 \times . Arrowheads indicate p65-positive cells. (B) Pulmonary p65-positive cells were counted. All data were expressed as means \pm SEM ($n = 12$). ** $P < 0.01$.

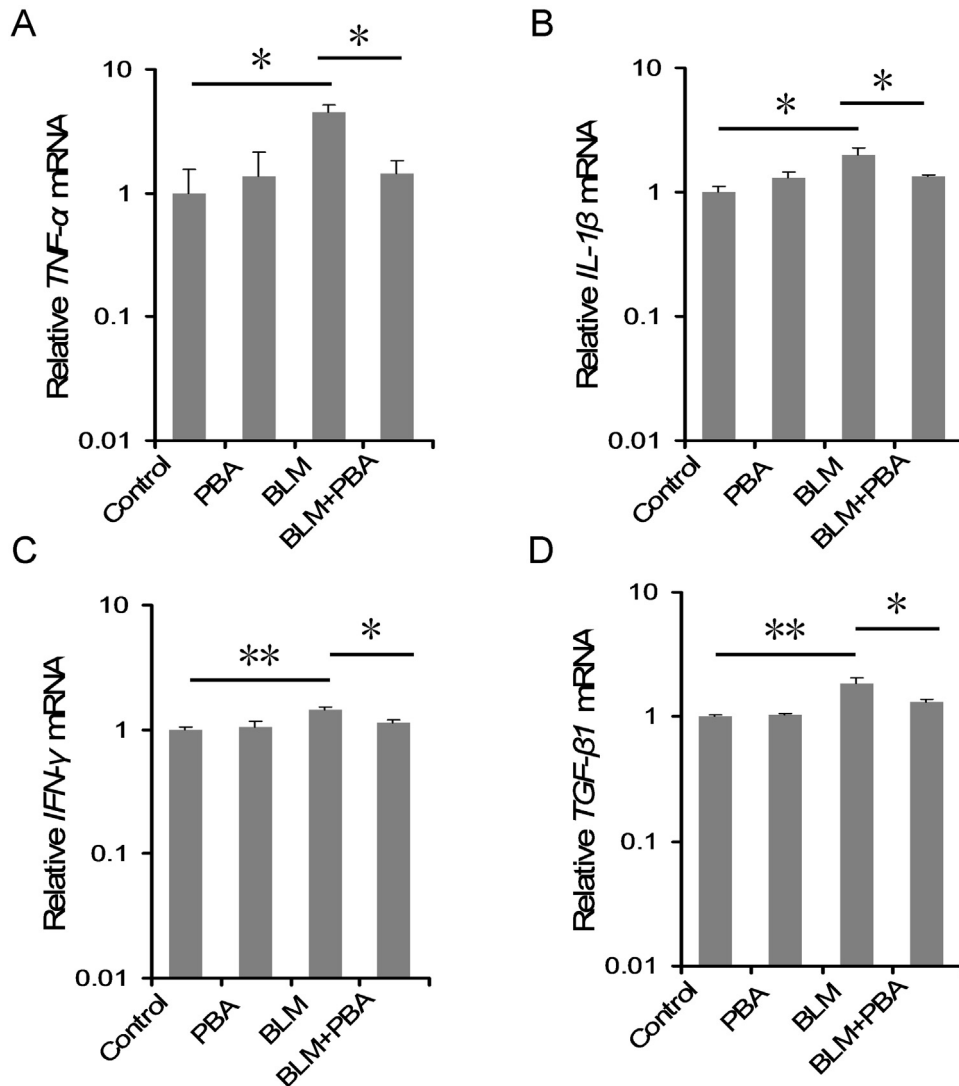


Fig. 4. Effects of PBA on BLM-induced pulmonary inflammatory cytokines. In BLM group, mice were intratracheally injected with a single dose of BLM (3.0 mg/kg body weight in 50 μ L phosphate buffered saline). In BLM + PBA group, mice were intratracheally injected with BLM in combination with PBA (150 mg/kg, i.p., daily). Lungs were collected 21 days after BLM. Pulmonary inflammatory cytokines were measured using real-time RT-PCR. (A) TNF- α ; (B) IL-1 β ; (C) IFN- γ ; (D) TGF- β 1. All data were expressed as means \pm SEM ($n = 12$). * $P < 0.05$, ** $P < 0.01$.

3.4. PBA inhibits BLM-induced up-regulation of pulmonary inflammatory cytokines

As shown in Fig. 4A–D, TNF- α , IL-1 β , IFN- γ and TGF- β 1, several inflammatory cytokines, were up-regulated in the lungs of BLM-treated mice. The effects of PBA on BLM-induced upregulation of pulmonary inflammatory cytokines were then analyzed. Consistent with its repression of NF- κ B activation, BLM-induced upregulation of pulmonary TNF- α , IL-1 β and IFN- γ was obviously inhibited by PBA (Fig. 4A–C). BLM-induced upregulation of pulmonary TGF- β 1, a major cytokine for induction of pulmonary EMT, was significantly repressed by PBA (Fig. 4D).

3.5. PBA inhibits BLM-induced EMT in the lungs

Alpha-SMA is a hallmark of myofibroblasts and is accepted as a marker of EMT. As shown in Fig. 5A and B, α -SMA was up-regulated in the lungs of BLM-treated mice. Immunohistochemistry showed that α -SMA-positive cells were significantly elevated in BLM-treated mice (Fig. 5C and D). PBA significantly inhibited BLM-induced up-regulation of α -SMA in the lungs (Fig. 5A and B).

Correspondingly, the number of α -SMA-positive cells in the lungs was significantly reduced in BLM + PBA-treated mice as compared with BLM-treated mice (Fig. 5C and D).

3.6. PBA alleviates BLM-induced pulmonary fibrosis

The hallmark characteristic of BLM-induced pulmonary fibrosis is excessive deposition of an extracellular matrix, such as collagen. As shown in Fig. 6A and B, the expression of pulmonary Col1 α 1 and Col1 α 2, two collagen genes, was significantly upregulated in BLM-treated mice. Correspondingly, an obvious matrix protein deposition, as evidenced by Sirius red staining, was observed in the lungs of BLM-treated mice (Fig. 6C and D). PBA significantly attenuated BLM-induced upregulation of Col1 α 1 and Col1 α 2 in the lungs (Fig. 6A and B). Moreover, PBA significantly alleviated BLM-induced matrix protein deposition in the lungs (Fig. 6C and D).

4. Discussion

The present study showed that pulmonary GRP78, an ER chaperone, was upregulated in BLM-treated mice. Moreover, the

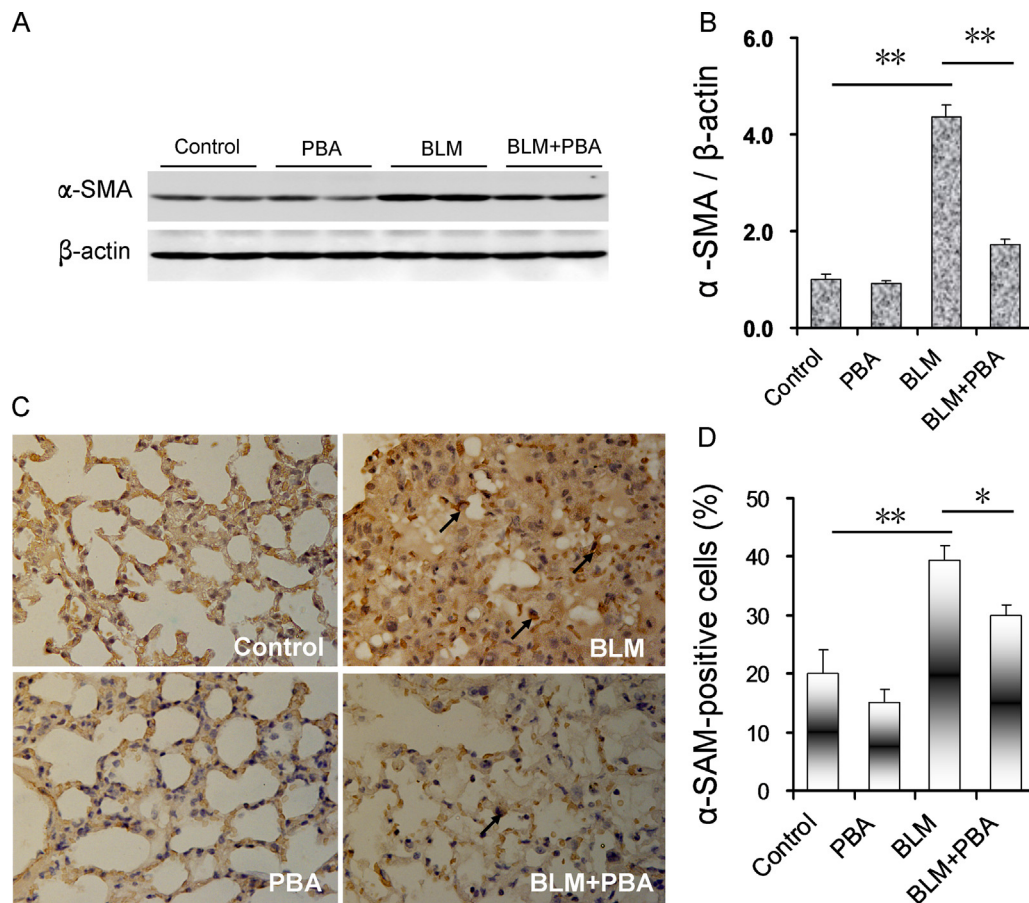


Fig. 5. Effects of PBA on BLM-induced pulmonary α -SMA expression. In BLM group, mice were intratracheally injected with a single dose of BLM (3.0 mg/kg body weight in 50 μ L phosphate buffered saline). In BLM + PBA group, mice were intratracheally injected with BLM in combination with PBA (150 mg/kg, i.p., daily). Lungs were collected 21 days after BLM. (A and B) The expression of pulmonary α -SMA was detected using immunoblots. All experiments were replicated for three times. (C and D) Pulmonary α -SMA was detected by immunohistochemistry. All experiments were replicated for four times. (C) Representative photomicrographs of pulmonary histological specimens from mice treated with saline, PBA alone, BLM alone and BLM plus PBA. Original magnification: 400 \times . Arrowheads indicate α -SMA-positive cells. (D) Pulmonary α -SMA-positive cells were counted. All data were expressed as means \pm SEM ($n=6$). * $P < 0.05$, ** $P < 0.01$.

level of CHOP, a downstream molecule of PERK signaling, was elevated in the lungs of BLM-treated mice. The level of phosphorylated eIF2 α , a downstream target of PERK signaling, was markedly elevated in the lungs of BLM-treated mice. In addition, phosphorylated IRE1 α in the lungs were markedly increased in BLM-treated mice. These results are in agreement with those from our recent study (Zhao et al., 2014), in which pulmonary phosphorylated IRE1 α and sXBP-1, a downstream molecule of IRE1 α signaling, were elevated in BLM-treated mice. In addition, the cleaved ATF6 in the nuclei and phosphorylated eIF2 α were increased in the lungs of BLM-treated mice (Zhao et al., 2014). These results suggest that the UPR signaling was activated in the pathogenesis of BLM-induced pulmonary fibrosis.

Increasing evidence indicates that PBA, an ER chemical chaperone, inhibits activation of the UPR signaling (Basseri et al., 2009; Hanada et al., 2007). Several studies showed that PBA effectively protected against cardiac fibrosis through alleviating ER stress (Ayala et al., 2012; Park et al., 2012). According to a report from our laboratory, PBA significantly attenuated CCl₄-induced hepatic ER stress and protected against CCl₄-induced liver fibrosis (Wang et al., 2013). Recently, a study demonstrated that PBA obviously repressed ER stress and prevented aortic fibrosis and stiffening in rats (Spitler and Webb, 2014). The present study investigated the effects of PBA on BLM-induced lung fibrosis in mice. We showed that PBA significantly attenuated BLM-induced ER stress and UPR activation in the lungs. Surprisingly, this ER

chemical chaperone significantly attenuated BLM-induced upregulation of pulmonary Col1 α 1 and Col1 α 2, two collagen genes. Moreover, PBA obviously alleviated BLM-induced matrix protein deposition in the lungs. These results suggest that PBA effectively protects against BLM-induced lung fibrosis in mice.

Numerous reports have demonstrated that EMT of alveolar epithelial cells to myofibroblasts plays a potential role in the pathogenesis of idiopathic pulmonary fibrosis (Willis et al., 2005). Indeed, several studies showed that pulmonary α -SMA, a hallmark of EMT to myofibroblasts, was upregulated during BLM-induced pulmonary fibrosis (Wang et al., 2013; Muro et al., 2008). According to two recent reports, pulmonary ER stress was involved in EMT in alveolar epithelial cells as a possible mechanism for fibrotic remodeling (Tanjore et al., 2011; Zhong et al., 2011). The present study investigated the effects of PBA on BLM-induced EMT in the lungs. We showed that pulmonary α -SMA expression was markedly upregulated in BLM-treated mice. Correspondingly, the number of α -SMA-positive cells in the lungs was significantly elevated in BLM-treated mice. PBA obviously inhibited BLM-induced EMT to myofibroblasts in the lungs, as evidenced by its repression of pulmonary α -SMA expression. Taken together, these results suggest that PBA protects against BLM-induced pulmonary fibrosis through its inhibition of EMT in the lungs.

The mechanism by which PBA inhibits pulmonary EMT remains obscure. Numerous studies have demonstrated that alveolar epithelial cells undergo EMT when chronically exposed to TGF-

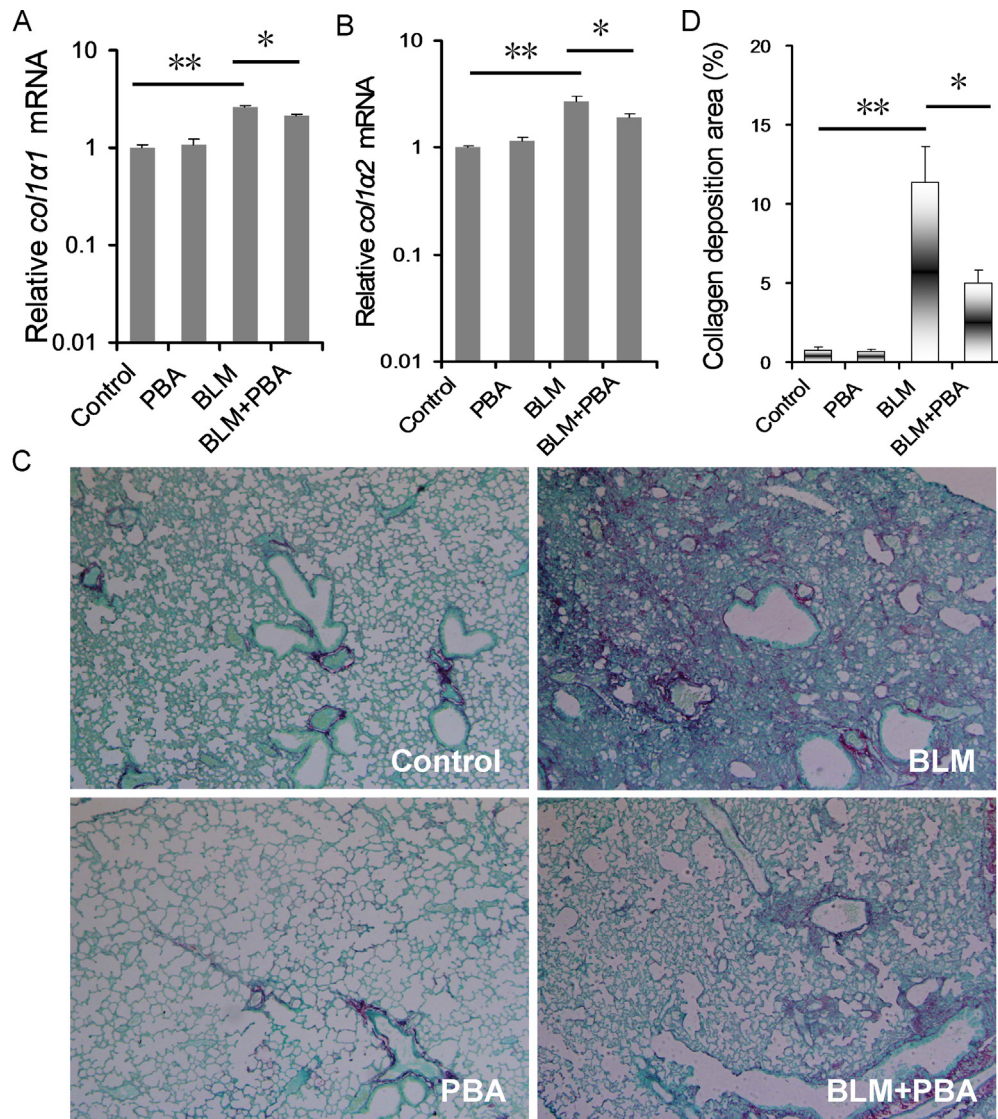


Fig. 6. Effects of PBA on BLM-induced pulmonary fibrosis. In BLM group, mice were intratracheally injected with a single dose of BLM (3.0 mg/kg body weight in 50 μ L phosphate buffered saline). In BLM + PBA group, mice were intratracheally injected with BLM in combination with PBA (150 mg/kg, i.p., daily). Lungs were collected 21 days after BLM. (A and B) The expression of pulmonary Col1 α 1 and Col1 α 2 was measured using real-time RT-PCR. (A) Col1 α 1; (B) Col1 α 2. (C and D) Lung fibrosis was evaluated by Sirius red staining. (C) Representative photomicrographs of pulmonary histological specimens from mice treated with saline, PBA alone, BLM alone and BLM plus PBA. Original magnification: 100 \times . (D) Collagen deposition areas were quantified. All data were expressed as means \pm SEM ($n = 6$). * $P < 0.05$, ** $P < 0.01$.

β 1 (Kim et al., 2006; Willis et al., 2005). On the other hand, according to a recent report, TNF- α accentuates TGF- β 1 driven EMT in primary bronchial epithelial cells (Borthwick et al., 2009). Indeed, the present study showed that the expression of TNF- α and TGF- β 1 in the lungs was significantly elevated in BLM-treated mice. Increasing evidence demonstrates that ER stress stimulates the expression of inflammatory cytokines through activation of NF- κ B signaling (Fougeray et al., 2011; Kim et al., 2013a,b). Moreover, PBA ameliorates LPS-induced lung inflammation through modulation of NF- κ B signaling (Kim et al., 2013a,b). The present study investigated the effects of PBA on BLM-induced NF- κ B activation and inflammatory cytokines in the lungs. We showed that BLM-induced activation of pulmonary NF- κ B signaling was inhibited by PBA. BLM-induced upregulation of pulmonary TNF- α and TGF- β 1 was accordingly attenuated by PBA. These results suggest that PBA partially alleviates BLM-induced upregulation of pulmonary inflammatory cytokines and subsequent EMT through modulation of NF- κ B signaling.

The present study laid emphasis on the effects of PBA on pulmonary inflammatory response and EMT in the pathogenesis of BLM-induced pulmonary fibrosis. However, the present study has several limitations. First, the present study only investigated the effects of a single dose PBA on BLM-induced EMT and pulmonary fibrosis. Second, the present study only investigated the effects of pretreatment with PBA on BLM-induced pulmonary fibrosis. Thus, additional work is required to determine a dose response curve to assess the effects of different doses PBA on BLM-induced EMT and pulmonary fibrosis. In addition, the anti-fibrotic effects of PBA need to be demonstrated in different models of pulmonary fibrosis.

In summary, the present study demonstrates that UPR signaling is activated in the pathogenesis of BLM-induced pulmonary fibrosis. PBA, a well-known ER chemical chaperone, inhibits BLM-evoked UPR activation in the lungs. Moreover, PBA alleviates BLM-induced pulmonary NF- κ B activation. In addition, PBA attenuates BLM-induced inflammatory response and subsequent EMT in the lungs. Importantly, PBA effectively protects against

BLM-induced lung fibrosis in mice. Thus, chemical chaperone may have potential preventive and therapeutic utilities for protecting against pulmonary fibrosis.

Conflict of interest

The authors have declared that there is no conflict of interest.

Transparency document

The [Transparency document](#) associated with this article can be found in the online version.

Acknowledgment

This work was supported by National Natural Science Foundation of China (3067178681001480).

References

- Adamson, I.Y., Bowden, D.H., 1974. The pathogenesis of bleomycin-induced pulmonary fibrosis in mice. *Am. J. Pathol.* 77, 185–197.
- Ayala, P., Montenegro, J., Vivar, R., Letelier, A., Urroz, P.A., Copaja, M., Pivet, D., Humeres, C., Troncoso, R., Vicencio, J.M., Lavandero, S., Díaz-Araya, G., 2012. Attenuation of endoplasmic reticulum stress using the chemical chaperone 4-phenylbutyric acid prevents cardiac fibrosis induced by isoproterenol. *Exp. Mol. Pathol.* 92, 97–104.
- Basseri, S., Lhotak, S., Sharma, A.M., Austin, R.C., 2009. The chemical chaperone 4-phenylbutyrate inhibits adipogenesis by modulating the unfolded protein response. *J. Lipid. Res.* 50, 2486–2501.
- Ben Mosbah, I., Alfany-Fernandez, I., Martel, C., Zaouali, M.A., Bintanel-Morcillo, M., Rimola, A., Rodes, J., Brenner, C., Rosello-Catafau, J., Peralta, C., 2010. Endoplasmic reticulum stress inhibition protects steatotic and non-steatotic livers in partial hepatectomy under ischemia-reperfusion. *Cell. Death. Dis.* 1, e52.
- Borchers, A.T., Chang, C., Keen, C.L., Gershwin, M.E., 2011. Idiopathic pulmonary fibrosis—an epidemiological and pathological review. *Clin. Rev. Allergy Immunol.* 40, 117–134.
- Borthwick, L.A., Parker, S.M., Brougham, K.A., Johnson, G.E., Gorowiec, M.R., Ward, C., Lordan, J.L., Corris, P.A., Kirby, J.A., Fisher, A.J., 2009. Epithelial to mesenchymal transition (EMT) and airway remodelling after human lung transplantation. *Thorax* 64, 770–777.
- Burlina, A.B., Ogier, H., Korall, H., Trefz, F.K., 2001. Long-term treatment with sodium phenylbutyrate in ornithine transcarbamylase-deficient patients. *Mol. Genet. Metab.* 72, 351–355.
- Fougeray, S., Bouvier, N., Beaune, P., Legendre, C., Anglicheau, D., Thervet, E., Pallet, N., 2011. Metabolic stress promotes renal tubular inflammation by triggering the unfolded protein response. *Cell. Death Dis.* 2, e143.
- Hanada, S., Harada, M., Kumemura, H., Bishr Omary, M., Koga, H., Kawaguchi, T., Taniguchi, E., Yoshida, T., Hisamoto, T., Yanagimoto, C., Maeyama, M., Ueno, T., Sata, M., 2007. Oxidative stress induces the endoplasmic reticulum stress and facilitates inclusion formation in cultured cells. *J. Hepatol.* 47, 93–102.
- Kim, K.K., Kugler, M.C., Wolters, P.J., Robillard, L., Galvez, M.G., Brumwell, A.N., Sheppard, D., Chapman, H.A., 2006. Alveolar epithelial cell mesenchymal transition develops in vivo during pulmonary fibrosis and is regulated by the extracellular matrix. *Proc. Natl. Acad. Sci. U. S. A.* 103 (13), 180–18185.
- Kim, H.J., Jeong, J.S., Kim, S.R., Park, S.Y., Chae, H.J., Lee, Y.C., 2013a. Inhibition of endoplasmic reticulum stress alleviates lipopolysaccharide-induced lung inflammation through modulation of NF-(B/HIF-1 α signaling pathway. *Sci. Rep.* 3, 1142.
- Kim, S.R., Kim, D.I., Kang, M.R., Lee, K.S., Park, S.Y., Jeong, J.S., Lee, Y.C., 2013b. Endoplasmic reticulum stress influences bronchial asthma pathogenesis by modulating nuclear factor κ B activation. *J. Allergy Clin. Immunol.* 132, 1397–1408.
- King, T.J., Pardo, A., Selman, M., 2011. Idiopathic pulmonary fibrosis. *Lancet* 378, 1949–1961.
- Kohno, K., 2007. How transmembrane proteins sense endoplasmic reticulum stress. *Antioxid. Redox Signal.* 9, 2295–2303.
- Lawson, W.E., Crossno, P.F., Polosukhin, V.V., Roldan, J., Cheng, D.S., Lane, K.B., Blackwell, T.R., Xu, C., Markin, C., Ware, L.B., Miller, G.G., Loyd, J.E., Blackwell, T.S., 2008. Endoplasmic reticulum stress in alveolar epithelial cells is prominent in IPF: association with altered surfactant protein processing and herpesvirus infection. *Am. J. Physiol. Lung Cell. Mol. Physiol.* 294, L1119–L1126.
- Lawson, W.E., Cheng, D.S., Degryse, A.L., Tanjore, H., Polosukhin, V.V., Xu, X.C., Newcomb, D.C., Jones, B.R., Roldan, J., Lane, K.B., Morrisey, E.E., Beers, M.F., Yull, F.E., Blackwell, T.S., 2011. Endoplasmic reticulum stress enhances fibrotic remodeling in the lungs. *Proc. Natl. Acad. Sci. U. S. A.* 108, 10562–10567.
- Moeller, A., Ask, K., Warburton, D., Gaudie, J., Kolb, M., 2008. The bleomycin animal model: a useful tool to investigate treatment options for idiopathic pulmonary fibrosis? *Int. J. Biochem. Cell. Biol.* 40, 362–382.
- Moore, B.B., Hogaboam, C.M., 2008. Murine models of pulmonary fibrosis. *Am. J. Physiol. Lung Cell. Mol. Physiol.* 294, L152–160.
- Muro, A.F., Moretti, F.A., Moore, B.B., Yan, M., Atrasz, R.G., Wilke, C.A., Flaherty, K.R., Martinez, F.J., Tsui, J.L., Sheppard, D., Baralle, F.E., Toews, G.B., White, E.S., 2008. An essential role for fibronectin extra type III domain A in pulmonary fibrosis. *Am. J. Respir. Crit. Care Med.* 177, 638–645.
- Ozcan, U., Yilmaz, E., Ozcan, L., Furuhashi, M., Vaillancourt, E., Smith, R.O., Gorgun, C. Z., Hotamisligil, G.S., 2006. Chemical chaperones reduce ER stress and restore glucose homeostasis in a mouse model of type 2 diabetes. *Science* 313, 1137–1140.
- Ozcan, L., Ergin, A.S., Lu, A., Chung, J., Sarkar, S., Nie, D., Myers Jr., M.G., Ozcan, U., 2009. Endoplasmic reticulum stress plays a central role in development of leptin resistance. *Cell. Metab.* 9, 35–51.
- Park, C.S., Cha, H., Kwon, E.J., Sreenivasaiah, P.K., Kim, D.H., 2012. The chemical chaperone 4-phenylbutyric acid attenuates pressure-overload cardiac hypertrophy by alleviating endoplasmic reticulum stress. *Biochem. Biophys. Res. Commun.* 421, 578–584.
- Spitler, K.M., Webb, R.C., 2014. Endoplasmic reticulum stress contributes to aortic stiffening via proapoptotic and fibrotic signaling mechanisms. *Hypertension* 63, e40–45.
- Tanjore, H., Cheng, D.S., Degryse, A.L., Zoz, D.F., Abdolrasulnia, R., Lawson, W.E., Blackwell, T.S., 2011. Alveolar epithelial cells undergo epithelial-to-mesenchymal transition in response to endoplasmic reticulum stress. *J. Biol. Chem.* 286, 30972–30980.
- Wang, J.Q., Chen, X., Zhang, C., Tao, L., Zhang, Z.H., Liu, X.Q., Xu, Y.B., Wang, H., Li, J., Xu, D.X., 2013. Phenylbutyric acid protects against carbon tetrachloride-induced hepatic fibrogenesis in mice. *Toxicol. Appl. Pharmacol.* 266, 307–316.
- Willis, B.C., Liebler, J.M., Luby-Phelps, K., Nicholson, A.G., Crandall, E.D., du Bois, R. M., Borok, Z., 2005. Induction of epithelial-mesenchymal transition in alveolar epithelial cells by transforming growth factor- β 1: potential role in idiopathic pulmonary fibrosis. *Am. J. Pathol.* 166, 1321–1332.
- Wu, J., Kaufman, 2006. From acute ER stress to physiological roles of the unfolded protein response. *Cell. Death Differ.* 13, 374–384.
- Xiao, C., Giacca, A., Lewis, G.F., 2011. Sodium phenylbutyrate, a drug with known capacity to reduce endoplasmic reticulum stress, partially alleviates lipid-induced insulin resistance and beta-cell dysfunction in humans. *Diabetes* 60, 918–924.
- Zhang, C., Chen, X., Zhu, R.M., Zhang, Y., Yu, T., Wang, H., Zhao, H., Zhao, M., Ji, Y.L., Chen, Y.H., Meng, X.H., Wei, W., Xu, D.X., 2012. Endoplasmic reticulum stress is involved in hepatic SREBP-1c activation and lipid accumulation in fructose-fed mice. *Toxicol. Lett.* 212, 229–240.
- Zhao, H., Wu, Q.Q., Cao, L.F., Qing, H.Y., Zhang, C., Chen, Y.H., Wang, H., Liu, R.R., Xu, D. X., 2014. Melatonin inhibits endoplasmic reticulum stress and epithelial-mesenchymal transition during bleomycin-induced pulmonary fibrosis in mice. *PLoS One* 9, e97266.
- Zhong, Q., Zhou, B., Ann, D.K., Minoo, P., Liu, Y., Banfalvi, A., Krishnaveni, M.S., Dubourd, M., Demaiio, L., Willis, B.C., Kim, K.J., DuBois, R.M., Crandall, E.D., Beers, M.F., Borok, Z., 2011. Role of endoplasmic reticulum stress in epithelial-mesenchymal transition of alveolar epithelial cells: effects of misfolded surfactant protein. *Am. J. Respir. Cell. Mol. Biol.* 45, 498–509.